

Document downloaded from:

<http://hdl.handle.net/10251/114623>

This paper must be cited as:

Ramirez Hoyos, P.; Cervera Montesinos, J.; Gómez Lozano, V.; Ali, M.; Nasir, S.; Ensinger, W.; Mafé, S. (2018). Optimizing Energy Transduction of Fluctuating Signals with Nanofluidic Diodes and Load Capacitors. *Small*. 14(18). doi:10.1002/sml.201702252



The final publication is available at

<http://doi.org/10.1002/sml.201702252>

Copyright John Wiley & Sons

#### Additional Information

This is the peer reviewed version of the following article: Ramirez Hoyos, P.; Cervera Montesinos, J.; Gómez Lozano, V.; Ali, M.; Nasir, S.; Ensinger, W.; Mafé, S. (2018). Optimizing Energy Transduction of Fluctuating Signals with Nanofluidic Diodes and Load Capacitors. *Small*. 14(18). doi:10.1002/sml.201702252, which has been published in final form at <http://doi.org/10.1002/sml.201702252>. This article may be used for non-commercial purposes in accordance with Wiley Terms and Conditions for Self-Archiving."

**DOI: 10.1002/ ((please add manuscript number))**

**Concept**

Optimizing energy transduction of fluctuating signals with nanofluidic diodes and load capacitors

*Patricio Ramirez, Javier Cervera, Vicente Gomez, Mubarak Ali, Saima Nasir, Wolfgang Ensinger, and Salvador Mafe\**

Prof. Dr. P. Ramirez, Dr. V. Gomez  
Departament. de Física Aplicada,  
Universitat Politècnica de València,  
E-46022 València, Spain

Dr. J. Cervera, Prof. Dr. S. Mafe  
Departament de Física de la Terra i Termodinàmica  
Universitat de València  
E-46100 Burjassot, Spain  
E-mail: Salvador.Mafe@uv.es

Dr. M. Ali, Dr. S. Nasir, Prof. Dr. W. Ensinger  
Department of Material- and Geo-Sciences  
Technische Universität Darmstadt  
D-64287 Darmstadt, Germany

Dr. M. Ali, Prof. Dr. W. Ensinger  
Materials Research Department  
GSI Helmholtzzentrum für Schwerionenforschung  
D-64291, Darmstadt, Germany.

Keywords: nanofluidic diodes, single and multipore membranes, fluctuating signals, iontronics, hybrid circuits, energy conversion

We consider the design and experimental implementation of hybrid circuits allowing charge transfer and energy conversion between nanofluidic diodes in aqueous ionic solutions and conventional electronic elements such as capacitors. The fundamental concepts involved are reviewed for the case of fluctuating zero-average external potentials acting on single pore and

multipore membranes. This problem is relevant to electrochemical energy conversion and storage, the stimulus-response characteristics of nanosensors and actuators, and the estimation of the accumulative effects caused by external signals on biological ion channels. Half-wave and full-wave voltage doublers and quadruplers can scale up the transduction between ionic and electronic signals. The network designs discussed here should be useful to convert the weak signals characteristic of the micro and nanoscale into robust electronic responses by interconnecting iontronics and electronic elements.

## 1. Introduction

In this concept article, we present hybrid circuits allowing charge transfer and energy conversion procedures between nanofluidic diodes in ionic solutions and conventional electronic elements such as capacitors. Also, we discuss the implications of the physical designs and experimental implementations described for future research. The references section is focused on the work reviewed and permits to explore other applications of the concept.

The physical approach is based on the efficient transduction between the ionic responses obtained at the micro- and nanoscale and the electronic readouts characteristic of the solid-state elements.<sup>[1-7]</sup> In particular, we have demonstrated the conversion of fluctuating zero-average external potentials into nonzero ionic currents, both in artificial<sup>[8-10]</sup> and biological<sup>[11,12]</sup> systems. These directional currents eventually produce robust electronic responses in hybrid networks with different interconnectivities submitted to white noise input signals.<sup>[13-16]</sup>

The conceptual problem is relevant to electrochemical energy conversion and storage procedures,<sup>[17,18]</sup> the quantification of the effects caused by external signals on biological ion

channels,<sup>[1,11,12]</sup> the study of the noisy responses characteristic of nanosensors and actuators,<sup>[5,7,19]</sup> and the ion pumping and desalination processes with conical nanopores.<sup>[20]</sup>

## 2. Hybrid Circuits with Nanopores and Load Capacitors

**Figure 1** shows the basic scheme for the electrical transduction of a fluctuating signal of zero-average into a net current that allows charging the load capacitor to significant voltages.<sup>[10,12]</sup> The process is experimentally robust and can be scaled up by using multipore membranes instead of single-nanofluidic diodes.<sup>[17]</sup> The hybrid network can be described theoretically by means of equivalent electrical circuits that permit to simulate the system response for each practical design.<sup>[16]</sup> We will focus here on the case of polymeric nanopores but the concepts developed can also be implemented using solid-state pores and ion channels.<sup>[4-7,11,12]</sup>

**Figure 2** shows four practical realizations<sup>[13-15]</sup> of the hybrid circuits based on nanofluidic diodes and load capacitors. The hybrid networks with the half-wave (HW) doubler, full-wave (FW) doubler, and HW quadrupler permit to scale up the energy conversion process of **Figure 1**. The characteristics of the different elements in the networks can be found elsewhere.<sup>[13-16,21,22]</sup> The single pore and multipore membranes incorporate ion tracks obtained from the irradiation of 12- $\mu\text{m}$  thick polyimide (PI) and polyethylene terephthalate (PET) foils at the linear accelerator UNILAC (GSI, Darmstadt) that are converted into approximately conical pores by asymmetric track-etching technique.<sup>[16,21,22]</sup>

The current ( $I$ )–potential ( $V$ ) curves of the resulting single pore<sup>[23]</sup> and multipore membranes<sup>[24]</sup> give pore radii in the ranges 10-40 nm (cone tip) and 300-600 nm (base). The  $I$ – $V$  curves measured in 0.1 M KCl aqueous solutions show also that the carboxylate residues on the pore surface are ionized at  $\text{pH} = 7$  (**Figure 2**).<sup>[25-27]</sup> These negative fixed charges are

inhomogeneously distributed along the conical pore and give the electrical rectification that allows the conversion of white noise input potentials into directional net currents.<sup>[10]</sup> Low pore resistances are obtained when the current enters the cone tip while high resistances are obtained when the current enters the base (**Figure 2**).<sup>[10]</sup>

### 3. Charge Transfer and Energy Conversion Applications

**Figure 3A** shows the experimental and simulated charging curves obtained as a function of time for the four practical realizations of **Figure 2** following the conceptual scheme of Figure 1. The cases of low (**Figure 3A**, left) and high (**Figure 3A**, right) fluctuating potential amplitudes are considered for a single pore membrane. **Figure 3B** shows the steady state capacitor voltages obtained using each scheme. In the case of low amplitudes the voltage doublers improve significantly the charging process with respect to the case of the simple charging process, where a stable steady voltage is hardly achieved. The use of the HW voltage quadrupler permits to obtain a steady voltage of *ca* 20 mV. For high amplitudes, stable steady voltages in the load capacitor are obtained for all schemes.

As expected, the capacitor voltage cannot reach the ideal values because of the limited rectification of the nanofluidic diodes (**Figure 2**). However, significant increases in the final voltages with respect to the simple charging are obtained in all cases. Furthermore, the results for the HW quadrupler suggest that other optimization procedures can be implemented by appropriate design of the hybrid networks. Remarkably, the experimental data can be described theoretically in terms of equivalent electrical circuits<sup>[14-16]</sup> that allow simple and accurate simulations of each network design.

**Figure 4** shows the steady state capacitor voltages obtained for the charging curves of **Figure 3** as a function of the fluctuating potential amplitude. **Figure 4A** corresponds to the single

pore case and is obtained with a load capacitor of capacitance  $C = 0.1 \mu\text{F}$ . **Figure 4B** corresponds to a multipore membrane and a capacitance  $C = 1.1 \text{ mF}$ . Note the significant increase in the steady state voltages that is obtained by using the voltage multipliers.

In reference 17, the energy stored in the load capacitor of capacitance  $C$  at the steady-state voltage reached at long times  $V(t \rightarrow +\infty) \equiv V_{\text{st}}$  was obtained as  $E_{\text{out}} = CV_{\text{st}}^2/2$ . This output energy can be compared with the input energy  $E_{\text{in}} = \int_0^{T=3\tau} I(t)\varepsilon(t)dt$ , where  $\varepsilon(t)$  is the randomly fluctuating electric potential,  $\tau$  is the characteristic time for charging and  $I(t)$  is the electrical current through the membrane. For a multipore membrane and a fluctuating potential amplitude of 2 V, the ratio between the above energies give the following efficiencies: 17 % (simple charging), 5.8 % (HW doubler), 9.5 % (FW doubler), and = 5.9 % (HW quadrupler) for  $C = 5 \text{ mF}$ . The FW doubler has a relatively short charging time compared with the HW doubler.

Note however that the above efficiencies depend on the fluctuating potential amplitude, the capacitance  $C$  and the individual nanofluidic diodes used. In particular, the efficiency obtained in the case of the HW quadrupler cannot be compared directly with the other cases because of the different four diodes used. In general, the use of multiple diodes reduces the efficiency with respect to the simple charging case at high voltages but avoids the significant fluctuations characteristic of the simple charging at low voltages. If the charging time is not a critical issue, the HW quadrupler can be used both at low and high voltages (the simple charging shows high output potential fluctuations at low voltages). However, if the charging time should be decreased, the simple charging can be used at high voltages.

**Figure 5** gives practical examples of energy conversion with single and multipore membranes in the cases of low and high fluctuating potential amplitudes. **Figure 5A** shows the scheme of the basic design. The capacitor is charged by the white noise rectification provided by the membrane with nanofluidic diodes (left). The stored electrical energy is used to feed a second membrane by allowing the capacitor to discharge (right), which may occur through the conductive or the non-conductive orientation of the nanofluidic diodes.

In **Figure 5B**, a single nanopore rectifies a low amplitude (300 mV) signal (**Figure 3A**, left) and the voltage of a load capacitor increases with time. The discharge of the capacitor is used to feed a second single pore membrane, producing the transient decrease shown in the capacitor voltage. Therefore, the energy stored during the simple charging allows an electrical current through the non-conductive (top curve) or conductive (bottom curve) orientation of another nanofluidic diode. **Figure 5C** demonstrates the same concept for the high amplitude (2 V) case (**Figure 3A**, right). **Figure 5D** corresponds again to a simple charging process but now the energy conversion occurs between two multipore membranes with pore densities  $10^4 \text{ cm}^{-2}$  (charging process) and  $10^3 \text{ cm}^{-2}$  (discharging process). The slow decrease observed in the capacitor voltage as the discharge proceeds through the second multipore membrane shows that the energy is transferred during a significant time period.

**Figure 5E** confirms further the validity of the concept for the case of a HW quadrupler-based charging process using the  $10^4 \text{ cm}^{-2}$  areal pore density membrane and the high amplitude signal. The discharge of the load capacitor with capacitance  $C = 1.1 \text{ mF}$  shown in the oscilloscope screen allows a LED diode to light up during a few seconds. This time can be significantly extended by using hybrid circuits with a higher equivalent capacitance at the price of increasing the charging time. However, the voltage multipliers are not intended to power this diode but to optimize the energy transduction of weak amplitude input signals with

nanofluidic diodes and enhance the stability of the resulting output signals (the load capacitor voltages here).

At this stage, the general concept emphasized is that networks of soft matter nanostructures can be electrically coupled to conventional electronic elements in signal transduction and energy conversion applications and that the feeding of an external circuit with a microdevice using the energy stored in the capacitor is feasible. In future designs, fluctuating signals from the ambient environment could be considered. In the case of thermal fluctuations or stochastic mechanical vibrations, for instance, appropriate transducers should be employed to convert first the input noises into fluctuating electrical signals. Alternatively, this intermediate step can be avoided by applying mechanical inputs (e.g., pressure pulses) directly to the nanofluidic diodes to obtain electrical responses as electromechanical effects.

Note also that hybrid circuits allow correcting for the mismatch between the electrical characteristics of nanopores and solid-state elements. Indeed, these systems are mismatched not only in their impedances but also in their operating voltages, especially in the case of biological nanopores (ion channels) whose typical voltages are of the order of  $kT/e = 27$  mV, where  $k$  is the Boltzmann constant,  $T$  is the absolute temperature, and  $e$  is the elementary charge.<sup>[12,28]</sup> **Figure 6A** shows a recent example concerning the rectification of fluctuating signals with a single protein ion channel (the outer membrane porin F protein, a bacterial channel of *Escherichia coli*) in a lipid bilayer. **Figure 6B** shows the experimental and theoretical charging curves obtained from the rectification of the white noise input potential. Note the low voltages characteristic of the biological ion channel (see Reference 12 for additional details) The design of hybrid circuits with voltage multipliers can bridge the operating voltages mismatch, as demonstrated recently for the case of an integrated biological–solid-state system.<sup>[28]</sup>



#### 4. Conclusion

We have reviewed fundamental concepts concerning the design and implementation of hybrid circuits consisting of nanofluidic diodes interconnected with conventional electronic elements such as capacitors. While emphasis has been put on charge transfer and energy transduction procedures, the conversion of white noise input signals into ionic responses at the micro and nanoscale that can eventually be processed as electronic signals has implications for future research because of the following facts:

(i) there exists a broad range of nanopore shapes and surface functionalizations that allow operation with different electrical, chemical, thermal, and optical input signals.<sup>[4-7,22-26]</sup> The basic concepts developed here can guide practical designs for processing these signals. In particular, for electrochemical energy conversion and storage<sup>[17,18,27]</sup> as well as for sensing and actuating with noisy stimuli that should eventually be translated into electronic readouts;<sup>[5,7,19,26]</sup>

(ii) the biological effects caused by external signals can be studied at the basic level of a single ion channel using the concepts developed here.<sup>[1,11,12]</sup> This approach may constitute a complementary method of studying the accumulative effects caused by external fields on the whole cell membrane. A detailed account of this application was given in reference 12;

(iii) there is an increasing interest in combining the capabilities of biological systems and solid state elements into hybrid devices, as shown recently for the case of integrated circuits powered by ATP-harvesting ion pumps.<sup>[28]</sup> The significant mismatch between the operating electric potentials characteristic of the basic circuit components<sup>[28]</sup> can be corrected by the use of voltage multipliers; and

(iv) future work may also address the spatial integration of the ionic circuits and hybrid networks<sup>[29]</sup> on microchips.<sup>[2,3,7,30,31]</sup> As an alternative to this scaling down, it is possible to design single micro and nanostructures that provide complex functionalities without interconnecting different single units.<sup>[7,23,32-37]</sup>

## **Acknowledgements**

P. R., J. C., V. G. and S. M. acknowledge the financial support from the Ministry of Economy and Competitiveness of Spain, (Materials Program, project No. MAT2015-65011-P), and FEDER. M.A., S.N. and W.E. acknowledge the funding from the Hessen State Ministry of Higher Education, Research and the Arts, Germany, under the LOEWE project iNAPO.

Received: ((will be filled in by the editorial staff))

Revised: ((will be filled in by the editorial staff))

Published online: ((will be filled in by the editorial staff))

## References

- [1] N. Misra, J. A. Martinez, S.-C. J. Huang, Y. Wang, P. Stroeve, C. P. Grigoropoulos, A. Noy, *Proc. Natl. Acad. Sci. U.S.A.* **2009**, *106*, 13780.
- [2] S. G. Lemay, *ACS Nano* **2009**, *3*, 775.
- [3] K. Tybrandt, K. C. Larsson, A. Richter-Dahlfors, M. Berggren, *Proc. Nat. Acad. Sci. U.S.A.* **2010**, *107*, 9929.
- [4] X. Duan, T.-M. Fu, J. Liu, C. M. Lieber, *Nano Today* **2013**, *8*, 351.
- [5] P. Ramirez, J. Cervera, M. Ali, W. Ensinger, S. Mafe, *ChemElectroChem* **2014**, *1*, 698.
- [6] W. Guan, S. Xin Li, M. A. Reed, *Nanotechnology* **2014**, *25*, 122001.
- [7] M. Tagliazucchi, I. Szleifer, *Mater. Today* **2015**, *18*, 131.
- [8] P. Ramirez, V. Gomez, M. Ali, W. Ensinger, S. Mafe, *Electrochem. Commun.* **2013**, *31*, 137.
- [9] V. Gomez, P. Ramirez, J. Cervera, S. Nasir, M. Ali, W. Ensinger, S. Mafe, *Appl. Phys. Lett.* **2015**, *106*, 073701.
- [10] V. Gomez, P. Ramirez, J. Cervera, S. Nasir, M. Ali, W. Ensinger, S. Mafe, *Sci. Rep.* **2015**, *5*, 9501.
- [11] M. Queralt-Martin, E. Garcia-Gimenez, V. M. Aguilera, P. Ramirez, S. Mafe, A. Alcaraz, *Appl. Phys. Lett.* **2013**, *103*, 043707.
- [12] C. Verdia-Baguena, V. Gomez, J. Cervera, P. Ramirez, S. Mafe, *PCCP* **2017**, *19*, 292.
- [13] V. Gomez, J. Cervera, S. Nasir, M. Ali, W. Ensinger, S. Mafe, P. Ramirez, *Electrochem. Commun.* **2016**, *62*, 29.
- [14] P. Ramirez, V. Gomez, C. Verdia-Baguena, S. Nasir, M. Ali, W. Ensinger, S. Mafe, *PCCP* **2016**, *18*, 3995.
- [15] P. Ramirez, V. Gomez, J. Cervera, S. Nasir, M. Ali, W. Ensinger, Z. Siwy, S. Mafe, *RSC Adv.* **2016**, *6*, 54742.
- [16] P. Ramirez, V. Garcia-Morales, V. Gomez, M. Ali, S. Nasir, W. Ensinger, S. Mafe, *Phys. Rev. Applied* **2017**, *7*, 064035.
- [17] P. Ramirez, V. Gomez, J. Cervera, S. Nasir, M. Ali, W. Ensinger, S. Mafe, *Nano Energy* **2015**, *16*, 375.
- [18] Y. Hou, R. Vidu, P. Stroeve, *Ind. Eng. Chem. Res.* **2011**, *50*, 8954.
- [19] M. Ali, I. Ahmed, P. Ramirez, S. Nasir, S. Mafe, C. M. Niemeyer, W. Ensinger, *Sensors Actuators B* **2017**, *240*, 895.
- [20] Y. Zhang, G. C. Schatz, *J. Phys. Chem. Lett.* **2017**, *8*, 2842.
- [21] P. Apel, *Radiat. Meas.* **2001**, *34*, 559.

- [22] Z. Siwy, L. Trofin, P. Kohli, L. A. Baker, C. Trautmann, C. R. Martin, *J. Am. Chem. Soc.* **2005**, *127*, 5000.
- [23] M. Ali, P. Ramirez, W. Ensinger, S. Mafe, *Appl. Phys. Lett.* **2012**, *101*, 133108.
- [24] J. Cervera, P. Ramirez, V. Gomez, S. Nasir, M. Ali, W. Ensinger, P. Stroeve, S. Mafe, *Appl. Phys. Lett.* **2016**, *108*, 253701.
- [25] S. Nasir, P. Ramirez, M. Ali, I. Ahmed, L. Fruk, S. Mafe, W. Ensinger, *J. Chem. Phys.* **2013**, *138*, 034709.
- [26] G. Pérez-Mitta, A. G. Albesa, C. Trautmann, M. E. Toimil-Molares, O. Azzaroni, *Chem. Sci.* **2017**, *8*, 890.
- [27] W. Guo, L. Cao, J. Xia, F.-Q. Nie, W. Ma, J. Xue, Y. Song, D. Zhu, Y. Wang, L. Jiang, *Adv. Funct. Mater.* **2010**, *20*, 1339.
- [28] J. M. Roseman, J. Lin, S. Ramakrishnan, J. K. Rosenstein, K. L. Shepard, *Nat. Commun.* **2015**, *6*, 10070.
- [29] P. Ramirez, V. Garcia-Morales, V. Gomez, M. Ali, S. Nasir, W. Ensinger, S. Mafe, *Phys. Rev. Applied* **2017**, in press.
- [30] G. Maglia, A. J. Heron, W. L. Hwang, M. A. Holden, E. Mikhailova, Q. Li, S. Cheley, H. Bayley, *Nat. Nanotechnol.* **2009**, *4*, 437.
- [31] J.-H. Han, K. B. Kim, H. C. Kim, T. D. Chung, *Angew. Chem. Int. Ed.* **2009**, *48*, 3830.
- [32] M. Ali, P. Ramirez, H. Q. Nguyen, S. Nasir, J. Cervera, S. Mafe, W. Ensinger, *ACS Nano* **2012**, *6*, 3631.
- [33] I. Vlassioux, Z. Siwy, *Nano Lett.* **2007**, *7*, 552.
- [34] J. Cervera, P. Ramirez, S. Mafe, P. Stroeve, *Electrochim. Acta* **2011**, *56*, 4504.
- [35] P. Ramirez, H. J. Rapp, S. Mafe, B. Bauer, *J. Electroanal. Chem.* **1994**, *375*, 101.
- [36] X. Hou, W. Guo, L. Jiang, *Chem. Soc. Rev.* **2011**, *40*, 2385.
- [37] W. Guo, Y. Tian, L. Jiang, *Acc. Chem. Res.* **2013**, *46*, 2834.

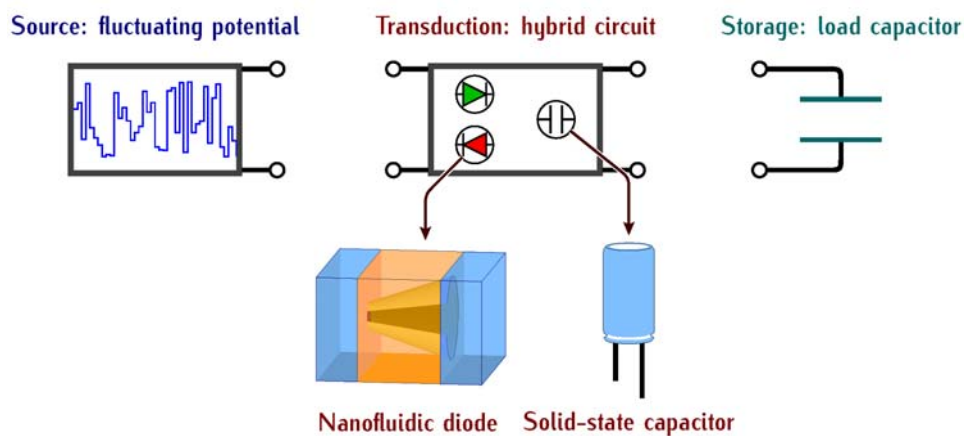


**Figure 1.** Scheme for the electrical transduction of a zero-average fluctuating signal that allows charging the load capacitor to significant voltages.<sup>[10,12]</sup> The charging process can be scaled up by using multipore membranes instead of a single nanofluidic diode.<sup>[17]</sup>

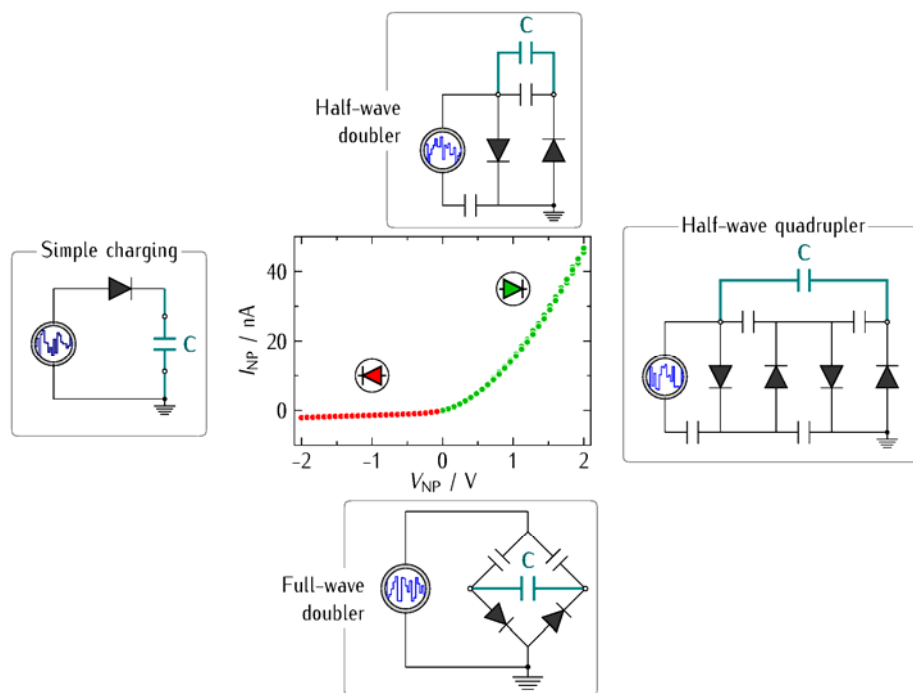


**Figure 2.** Four practical realizations<sup>[13-15]</sup> of hybrid circuits based on nanofluidic diodes and load capacitors. The electrical rectification shown by the current ( $I$ )–potential ( $V$ ) curve of a single nanofluidic diode (center) allows the conversion of white noise input potentials into net currents.<sup>[10]</sup> These currents permit to charge a load capacitor (simple charging process). The hybrid networks with the half-wave (HW) doubler, full-wave (FW) doubler, and HW quadrupler shown schematically permit to scale up the energy conversion.

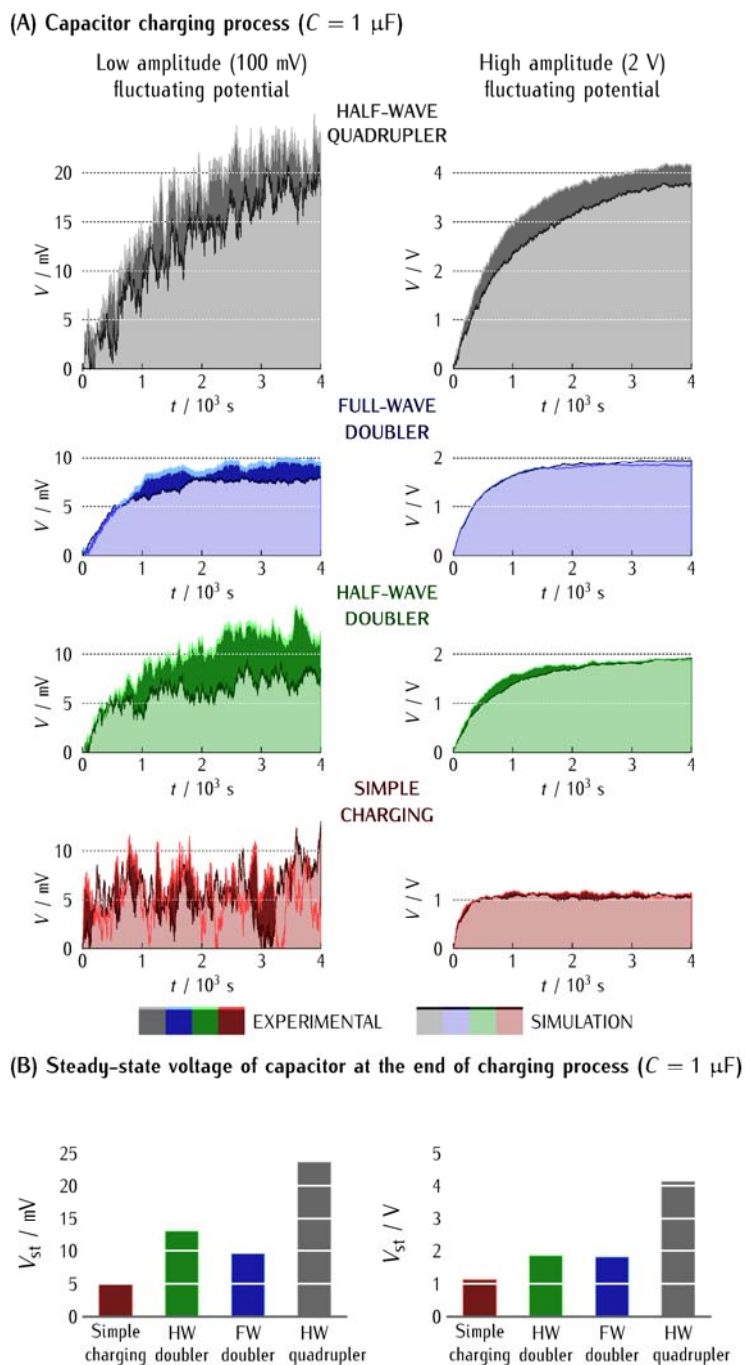


**Figure 3.** (A) The experimental and simulated capacitor charging curves obtained with the four practical realizations of Figure 2 and a single pore membrane. The cases of low (left) and high (right) fluctuating potential amplitudes are considered. (B) The steady state capacitor voltages  $V_{st}$  obtained at long times from the time-dependent charging curves for the cases of the simple charging, HW and FW doublers, and HW quadrupler. The simulations are carried out using equivalent electrical circuits for each network design.<sup>[14-16]</sup>

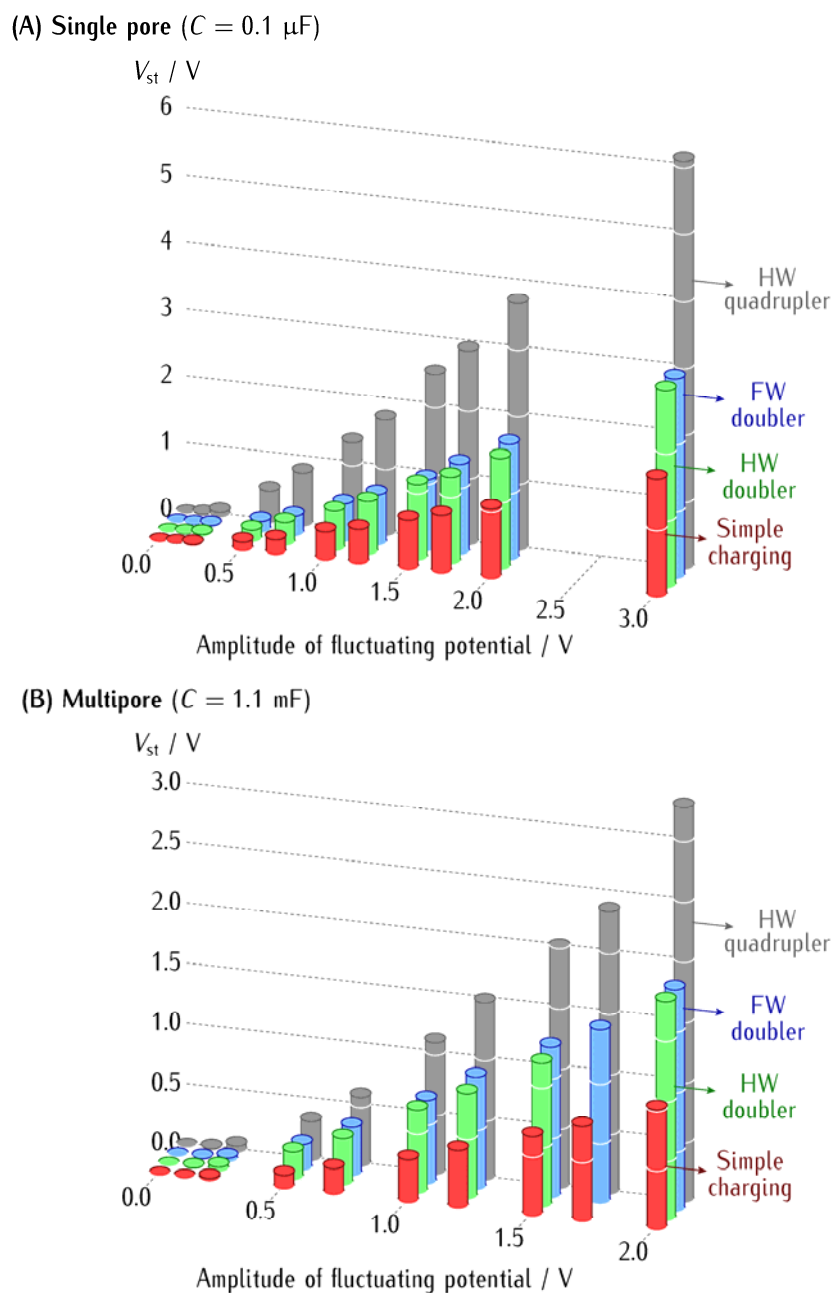


**Figure 4.** (A) Steady state capacitor voltages as a function of the fluctuating voltage amplitude for the single pore case and a load capacitor of capacitance  $C = 0.1 \mu\text{F}$ . (B) Steady state capacitor voltages as a function of the fluctuating voltage amplitude for the multipore membrane case and a capacitance  $C = 1.1 \text{ mF}$ .



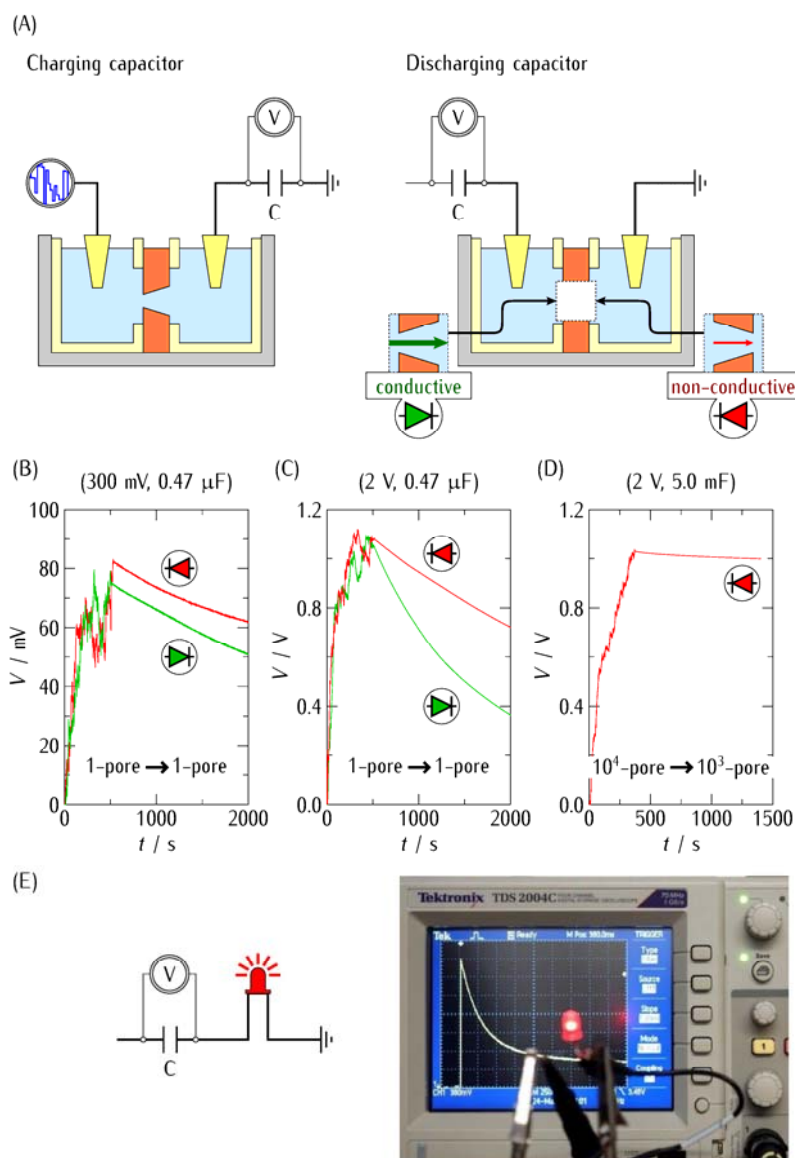


**Figure 5.** (A) Scheme of the basic design and elements considered in the charging (left) and discharging (right) capacitor experiments. In the second case, the discharging may occur through the conductive or the non-conductive orientation of the nanofluidic diodes. (B) A low amplitude (300 mV) signal is rectified by a first single nanopore. The voltage of a load capacitor of capacitance  $C = 0.47 \mu\text{F}$  increases with time (first part of the curve). The energy stored during the charging allows an electrical current through a second single nanopore during the capacitor discharging, which gives the decrease observed in the capacitor voltage (second part of the curve). The discharging may proceed either through the non-conductive (top curve) or through the conductive (bottom curve) orientation of the nanofluidic diode. (C) A similar experiment can also be conducted for the case of a high amplitude (2 V) signal. (D) The simple charging process due to the rectification of a multipore PI membrane with pore density  $10^4 \text{ cm}^{-2}$  allows charging a load capacitor of capacitance  $C = 5.0 \text{ mF}$  (first part of the curve). The capacitor discharging (second part of the curve) proceeds through a multipore PET membrane with pore density  $10^3 \text{ cm}^{-2}$ , which gives the slow decrease observed in the capacitor voltage. (E) A HW quadrupler circuit based on the  $10^4 \text{ cm}^{-2}$  PI membrane operated in the high amplitude case allows charging a capacitor of  $C = 1.1 \text{ mF}$ . The discharging curve of this capacitor shown in the oscilloscope screen permits the LED diode to light up.

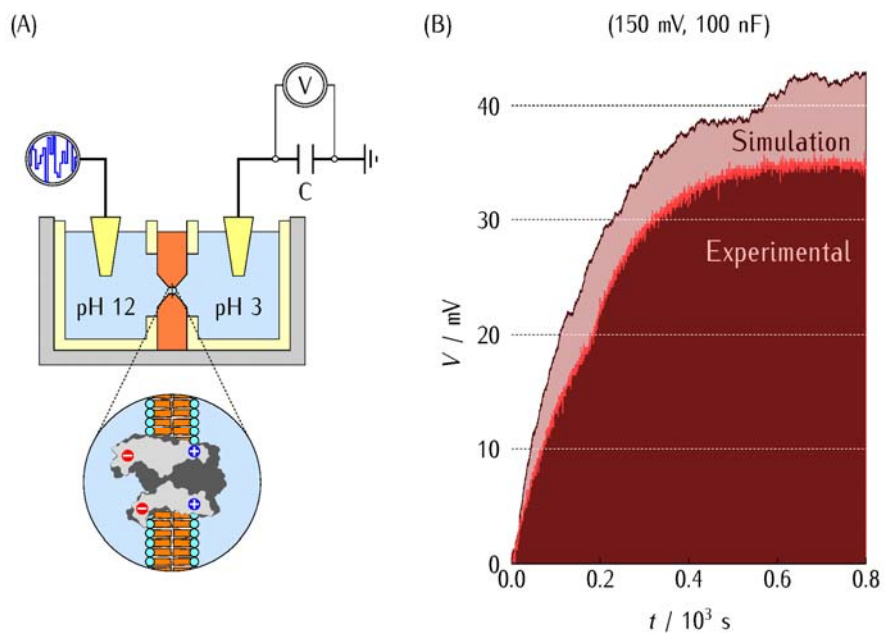


**Figure 6.** (A) Scheme of the rectification of an input white noise signal using a single protein ion channel (the outer membrane porin F protein, *OmpF*) in a lipid bilayer. (B) The experimental and simulated charging curves corresponding to a capacitor of capacitance  $C = 100$  nF are obtained for a fluctuating potential of amplitude 150 mV.<sup>[12]</sup>

**Nanofluidic diodes incorporated in single and multipore membranes allow the transduction of zero-average fluctuating signals into directional net currents that can be stored in load capacitors.** This concept permits to design hybrid circuits for energy conversion processes.

**Keyword:** nanofluidic diodes, single and multipore membranes, fluctuating signals, iontronics, hybrid circuits, energy conversion

Patricio Ramirez, Javier Cervera, Vicente Gomez, Mubarak Ali, Saima Nasir, Wolfgang Ensinger, and Salvador Mafe\*

**Title** Optimizing energy transduction of fluctuating signals with nanofluidic diodes and load capacitors

ToC figure ((Please choose one size: 55 mm broad × 50 mm high **or** 110 mm broad × 20 mm high. Please do not use any other dimensions))

